The Goblet Cell Protein Clca1 (Alias mClca3 or Gob-5) Is Not Required for Intestinal Mucus Synthesis, Structure and Barrier Function in Naive or DSS-Challenged Mice

Nancy A. Erickson[1]☯, Elisabeth E. L. Nyström[2]☯, Lars Mundhenk[1], Liisa Arike[2], Rainer Glauben[3], Markus M. Heimesaat[4], André Fischer[4], Stefan Bereswill[4], George M. H. Birchenough[2], Achim D. Gruber[1]‡, Malin E. V. Johansson[2]‡*

1 Department of Veterinary Pathology, Freie Universität Berlin, Berlin, Germany, **2** Department of Medical Biochemistry, University of Gothenburg, Gothenburg, Sweden, **3** Medical Department, Division of Gastroenterology, Infectiology and Rheumatology—Charité, Universitätsmedizin Berlin, Berlin, Germany, **4** Department of Microbiology and Hygiene, Charité - Universitätsmedizin Berlin, Berlin, Germany

☯ These authors contributed equally to this work.
‡ These authors contributed equally as senior authors on this work.
* malin.johansson@medkem.gu.se

Abstract

The secreted, goblet cell-derived protein Clca1 (chloride channel regulator, calcium-activated-1) has been linked to diseases with mucus overproduction, including asthma and cystic fibrosis. In the intestine Clca1 is found in the mucus with an abundance and expression pattern similar to Muc2, the major structural mucus component. We hypothesized that Clca1 is required for the synthesis, structure or barrier function of intestinal mucus and therefore compared wild type and *Clca1*-deficient mice under naive and at various time points of DSS (dextran sodium sulfate)-challenged conditions. The mucus phenotype in *Clca1*-deficient compared to wild type mice was systematically characterized by assessment of the mucus protein composition using proteomics, immunofluorescence and expression analysis of selected mucin genes on mRNA level. Mucus barrier integrity was assessed *in-vivo* by analysis of bacterial penetration into the mucus and translocation into sentinel organs combined analysis of the fecal microbiota and *ex-vivo* by assessment of mucus penetrability using beads. All of these assays revealed no relevant differences between wild type and *Clca1*-deficient mice under steady state or DSS-challenged conditions in mouse colon. Clca1 is not required for mucus synthesis, structure and barrier function in the murine colon.

Introduction

The goblet-cell derived protein Clca1 (chloride channel regulator, calcium-activated-1, previously termed mClca3 or gob-5, see revised nomenclature S1 Table) has repeatedly been linked

to several human respiratory conditions such as asthma, cystic fibrosis (CF) and chronic obstructive pulmonary disease (COPD) as well as to corresponding mouse models [1–4]. Common features related to disease severity are goblet cell hyperplasia, mucus overproduction and disturbed clearance, together with Clca1 protein and mRNA overexpression which has led to the conclusion that Clca1 is involved in mucin gene expression and/or altering mucus properties [4]. Experimental overexpression of murine Clca1 aggravates the asthma phenotype in ovalbumin- or interleukin (IL)-9-challenged mouse models [5,6]. Conversely, neutralization via antisense- or antibody-treatment of Clca1 ameliorates disease severities [5,7].

Indeed, it was recently shown that the human CLCA1 induces airway goblet cell metaplasia via an extracellular MAPK (mitogen-activated protein kinase)-signaling pathway that drives mucus gene expression [8]. Therefore, CLCA1 may be key to the pathogenesis of conditions with mucus overproduction, possibly suggesting a role in novel therapeutic concepts [4]. However, the function of CLCA1 is still far from being understood.

CLCA1 is abundantly secreted by goblet cells of the intestinal tract together with the MUC2 mucin [9–13]. MUC2 is a highly glycosylated, multimerizing protein and the main structural mucus component, creating net-like sheets that stack upon each other after secretion, thus forming a sieving mucus structure that is normally impenetrable to bacteria [11,14]. It thereby acts as a protective gel, providing an effective barrier against the commensal colonic bacteria [11,15]. In patients with ulcerative colitis, there is strong evidence for mucus layer disruption contributing to the disease pathogenesis [16]. Also, experimentally altered mucus properties consistently induce colitis in mice due to breakdown of the intestinal mucus barrier [16–18].

Several other proteins have been identified in the mucus which are thought to also contribute to mucus structure formation [11,13]. One of these is Clca1, a major constituent of the extracellular intestinal mucus, with a similar expression pattern to Muc2 along the intestinal axis [13]. During its biosynthesis, the primary Clca1 translation product is autocatalytically cleaved within its carboxy-terminal region into two secreted cleavage products by a self-contained zinc-dependent metallohydrolase [19–22]. Such metallohydrolases are thought to critically alter mucus properties [23]. Additionally, a conserved von Willebrand factor type A (vWA) domain with a metal-dependent adhesion site is contained in the amino-terminal cleavage product of CLCA1 which implies that it may interact with other proteins [20,24,25], supporting the notion of a structural role in mucus formation. Furthermore, restoration of decreased Clca1 protein levels in a mouse model of CF has been shown to ameliorate intestinal mucus plugging which is a common trait of human and murine CF [23,26]. It has consequently been hypothesized that CLCA1 may play a role in mucus formation [5,10,21,24,27].

In this study we characterized the intestinal mucus phenotype and microbiota composition of wild type (WT) versus *Clca1*-deficient (*Clca1*⁻/⁻) mice under naive conditions, in a set of *ex vivo* experiments and under conditions of DSS (dextran sodium sulfate) challenge. DSS destabilizes biophysical mucus layer properties but is thought not to affect mucin biosynthesis [28]. It is commonly used to experimentally induce colitis via its rapid deleterious effects on mucus integrity which causes mucus barrier disruption and allows bacterial penetration and subsequent epithelial barrier disruption [28,29]. The consequent inflammatory response results in clinically manifest colitis after a treatment course of several days that in many ways resemble and can be used as a model for Ulcerative colitis [29]. Here, mucus barrier integrity was also determined by quantification of bacterial translocation into sentinel organs. Furthermore, the intestinal microbiota composition was analyzed in terms of main gut bacterial groups since these are known to be sensitively altered during development of experimental colitis [30,31].

Much to our surprise, we failed to detect any differences in all of our experimental readout parameters between *Clca1*⁻/⁻ and wild type mice, regardless of whether unchallenged or DSS-challenged tissues were employed.

Materials and Methods

Ethics statement, mice and DSS treatment

All animal studies involving naive mice were conducted at the Department of Medical Biochemistry, University of Gothenburg, Sweden, in full compliance with Swedish animal welfare legislation and approved by the Swedish Laboratory Animal Ethical Committee in Gothenburg, Sweden (number: 280–2012). Animal studies also involving DSS treatment were conducted at the Research Institutes for Experimental Medicine, Charité - Universitätsmedizin Berlin, Campus Benjamin Franklin, Germany, in strict accordance with the FELASA guidelines and recommendations for the care and use of laboratory animals [32] and approved by the local governmental authorities (State Office of Health and Social Affairs Berlin, approval IDs: T 0394/12; G 0170/12).

Naive *Clca1*^{−/−} mice, generated on a C57BL/6J background [33] and control mice of the same genetic background were allowed an acclimatization period of at least 10 days and housed under standardized SPF conditions. Animals of both genders between 6 and 12 weeks of age were used, except for DSS experiments involving only weight- and age-matched female mice. For experimental procedures, mice were given 2.5% DSS (MW 36,000–50,000, 17.1% sulfur substitution, no detectable free sulfate, pH 7.1, MP Biomedicals, LLC., Illkirch, France) in their drinking water for 24 (24 h-group) or 48 (48 h-group) hours to allow for the investigation of initial mucus barrier disruptions. In addition, DSS administration for 7 days with 2 consecutive days of tap water only (7 d-group) allowed the monitoring of effects with a completely disrupted barrier and assessment of clinical parameters in terms of fecal blood content [34], using the hemoCARE Guaiac testing method (CARE diagnostic, Voerde, Germany) and stool consistency [35]. All mice were anesthetized with isoflurane prior to euthanasia by cervical dislocation.

Immunofluorescence

Intestinal tissues were fixed in Methanol-Carnoy and immunostained as described before [36]. Sections were immunostained with a rabbit anti-MUC2-C3 antibody (1:500) [11] and co-stained with a mouse anti-human CLCA1 antibody (Abcam, Cambridge, UK, ab129283, 1:1,000). Goat anti-rabbit IgG conjugated to Alexa Fluor 488 (Molecular Probes, Thermo Fisher, Waltham, MA USA, 1:1,000), or goat anti-mouse IgG conjugated to Alexa Fluor 546 (Molecular Probes, Thermo Fisher, 1:1,000) were used as secondary antibodies, respectively. WT and *Clca1*^{−/−} intestinal sections were stained with a rabbit anti-mouse CLCA1 antibody (amino-terminal reactive; Abcam ab46512, 1:1,000) or a mouse anti-human CLCA1 antibody (carboxy-terminal reactive; Abcam ab129283, 1:2,000) combined with an appropriate Alexa Fluor 546-conjugated secondary antibody to verify the antibody specificity. Other primary antibodies used were: goat anti-Agr2 (Santa Cruz Biotechnology, Dallas, USA, sc-54561, 1:100), rabbit anti-Fcgbp (Sigma-Aldrich, HPA003517, 1:100), rabbit anti-Klk1 (Boster Immunoleader, Pleasanton, CA, PA1709, 1:1,000) or rabbit anti-Zg16 (made in house, PH8292B-11, 1:600) [13] followed by the appropriate Alexa Fluor 546-conjugated secondary antibodies. DNA was stained for 5 min using 1 µg/ml Hoechst 34580 (Molecular Probes, Thermo Fisher). Micrographs were obtained using a Nikon eclipse E1000 fluorescence microscope (Nikon, Tokyo, Japan) with the NIS elements software (Nikon) or a LSM700 Axio Examiner Z.1 confocal microscope (Zeiss, Göttingen, Germany) with the ZEN 2010 software (Zeiss).

Proteomics

Sample collection. Mucus samples were collected from flushed colonic tissue of WT and *Clca1*^{−/−} mice mounted in a horizontal perfusion chamber as described for mucus thickness measurements below but without removal of the muscle layer. 10 µm polystyrene beads

(FluoSpheres, Molecular Probes, Thermo Fisher) were used to visualize the mucus layer. Mucus was gently scraped off the epithelium into the apical buffer and was collected using a micropipette [37]. 2x cOmplete EDTA (ethylenediaminetetraacetic acid)-free protease inhibitor (Roche, Mannheim, Germany) was added to the samples.

Sample preparation. Mucus samples were incubated overnight at 37°C in reduction buffer (6 M GuHCl, 0.1 M Tris/ HCl pH 8.5 (Merck), 5 mM EDTA, 0.1 M DTT (Merck)) followed by a FASP (Filter-aided Sample Prep) digestion protocol [38] using 6 M guanidinium hydrochloride (GuHCl) instead of urea. Briefly, proteins were alkylated on 30 kDa cut-off filters and subsequently digested for 4 h with LysC (Wako, Richmond, VA, USA) followed by an overnight trypsin (Promega, Fitchburg, WI, USA) digestion. Peptides released from the filter after centrifugation were cleaned with StageTip C18 columns as previously described [13,39].

Nano-Liquid-Chromatography Mass-spectrometry (NanoLC–MS/MS). NanoLC–MS/MS was performed on an EASY-nLC system (Thermo Scientific, Odense, Denmark), connected to a Q Exactive Hybrid Quadrupole-Orbitrap Mass Spectrometer (Thermo Scientific) through a nanoelectrospray ion source. Peptides were separated with reverse-phase column (150 × 0.075 mm inner diameter, C18-AQ 3 μm) by 95-minute gradient from 5 to 30% B A (A: 0.1% formic acid, B: 0.1% formic acid/80% acetonitrile 200 nl/min). Full mass spectra were acquired from 350–1,600 m/z with resolution of 70,000 (m/z 200). Up to twelve most intense peaks (charge state $\geq$ 2) were fragmented and tandem mass spectrum was acquired with a resolution of 35,000 and dynamic exclusion 30 s.

Data analysis. Data was analyzed with the MaxQuant program (version 1.4.1.2 [40]), as previously described [13].

Label-free quantification was performed by loading LFQ-intensity data from the MaxQuant output to the Perseus software (version 1.4.1.3). The data was filtered based on the presence of a protein group in at least four out of five samples in at least one group. Each group (WT and *Clca1*^{-/-} mice) was averaged using the median with the median values being presented in a scatterplot.

The mass spectrometry proteomics data were deposited to the ProteomeXchange Consortium (http://proteomecentral.proteomexchange.org) via the PRIDE partner repository [41] with the dataset identifier PXD001804.

Mucus thickness measurements and responsiveness to induced secretion

Procedure, material and equipment were employed as previously described [37]. Briefly, the distal colon was dissected and thoroughly flushed with ice-cold, oxygenated Krebs' solution. It was then opened up and the longitudinal muscle layer removed before being mounted in a 2.5 mm horizontal perfusion chamber with oxygenated basolateral Krebs' glucose solution and apical Krebs' mannitol solution. Activated charcoal particles (Fluka) were added to the apical surface to visualize the mucus layer. The mucus thickness was measured every 15 min for 1 h after an initial measurement at time 0 h (t0). To investigate the responsiveness of the tissue to induce mucus secretion, carbachol (CCh, 1mM, Sigma Aldrich) was added to the basolateral buffer after 30 min in one of the two specimen-containing chambers.

Mucus penetrability assay

The mucus penetrability assay was performed on distal colon tissue as previously described [16,37]. Briefly, the colonic explants were mounted in the perfusion chamber with basolateral Kreb's glucose solution containing 1μg/ml Calcein violet tissue stain (CellTrace Calcein Violet, Molecular Probes, Thermo Fisher) and a suspension of far red fluorescent beads (FluoSpheres

Carboxylate-Modified Microspheres, 1.0 μm, red fluorescent (580/605), 2% solids, Molecular Probes, Thermo Fisher) and Kreb's mannitol solution was added to the apical side and allowed to sediment for 5 min before it was refilled with Kreb's mannitol solution. The distribution of the beads in the mucus was investigated by acquiring confocal images in XY stacks (320 x 320 μm) 30min after tissue mounting. These were obtained using a LSM700 Axio Examiner Z.1 confocal microscope with Plan-Apochromat x 20/1.0 DIC water objective (Zeiss) and the ZEN 2010 software (Zeiss). Average bead distance from the tissue surface was calculated by combining bead fluorescence intensity data for each z-plane above the tissue surface.

Fluorescence-*in situ*-hybridization

This was performed as previously described [36]. In brief, de-waxed and washed Methanol-Carnoy fixed tissues were hybridized with the general bacterial probe, EUB338-I (250 ng, 5′ – GCT GCC TCC CGT AGG AGT–3′ , Eurofins genomics, Ebersberg, Germany), conjugated to Alexa Fluor 555 (Molecular Probes, Thermo Fisher) [11,36]. For mucus visualization slides were incubated with a rabbit anti-MUC2-C3 antibody (1:500) followed by incubation with goat anti-rabbit IgG conjugated to Alexa Fluor 488 (1:1000, Molecular Probes, Thermo Fisher). Nuclei were stained with Hoechst 34580 (Molecular Probes, Thermo Fisher) at 1 μg/ml in PBS. Slides were dried and cover-slipped with ProLong Antifade (Molecular Probes, Thermo Fisher). Micrographs were obtained using an Eclipse E1000 (Nikon) fluorescence microscope with the NIS element software (Nikon).

Mucus penetration, mucus layering and goblet cell filling score

Bacterial penetration of the inner mucus layer was scored using the fluorescence-*in situ*-hybridization (FISH)-, anti-Muc2- and DNA-stained sections as described previously (S2 Table) [28]. The mucus layering score, focusing solely on the layering and structure of the inner, stratified mucus layer and the goblet cell filling score [16] were applied (S3 Table and S4 Table, respectively). Sections were scored independently by two blinded individuals, except for the naive controls which were scored by one blinded individual using the Eclipse E1000 and Eclipse90i (Nikon) fluorescence microscope as well as the Axiovert 200M microscope (Zeiss) with the EXFO X-Cite 120 Fluorescence Illumination System (Olympus, Hamburg, Germany). Micrographs were obtained using the LSM700 Axio Examiner Z.1 confocal microscope (Zeiss) with the ZEN 2010 software (Zeiss).

Bacterial translocation

Blood derived via sterile cardiac puncture and biopsies of spleen, liver and mesenteric lymph-nodes (MLN) draining the large intestine were taken from WT and *Clca1*^-/- controls under naive conditions as well as after DSS challenge (7 d-group; n = 10 per group) and cultivated in thioglycolate enrichment broths (Thioglycolat-Bouillon, Oxoid, Wesel, Germany) as described [42]. Bacterial growth was monitored daily by turbidity assessment. Aliquots from turbid broths were cultivated on solid media under aerobic, microaerophilic and obligate anaerobic conditions and the bacterial species were identified microbiologically and biochemically as described earlier [43].

Fecal microbiota composition—Real-time PCR and quantification of 16S rRNA gene sequences

Real-time PCR-based quantification of main gut bacterial groups—*Enterobacteriaceae*, Entero-cocci, lactic acid bacteria, bifidobacteria, *Bacteroides/ Prevotella spp.*, *Clostridium leptum*

group, *Clostridium coccoides* group, mouse intestinal bacteroidetes and total eubacterial load—was performed.

DNA was extracted from colonic fecal samples as described previously (Heimesaat 2006) with minor modifications. Here, the sediment was incubated with 50 µl of lysozyme (20 mg/ml) and proteinase K (20 mg/ml; Sigma-Aldrich) for 30 min at 37°C and resuspended with 0.5 ml of lysis buffer (0.01 M Tris pH 9.0, 0.02 M EDTA, 0.15 M NaCl, 0.5% SDS).

Total DNA was quantified via Quant-iT PicoGreen dsDNA reagent (Invitrogen, Paisley, UK) as described [44] and adjusted to 10 ng DNA/µl. The abundance of specific intestinal bacterial groups was measured by quantitative real-time PCR as described [42,44–46]. Targets and 16S rRNA gene group-specific primers are listed in S5 Table. Data are expressed as median in a scatterplot. A minimum cut-off value of 10^0 gene copy numbers/ng DNA and a minimum log-change of 1 were set as limits of statistically significant relevance with $p < 0.05$.

RNA isolation and quantitative reverse transcriptase-qPCR

Sections of the distal colon were opened longitudinally, flushed briefly in ice-cold PBS before snap freezing in liquid nitrogen for subsequent storage at -80°C. Total RNA isolation using the Nucleo Spin RNA isolation Kit (Macherey Nagel, Düren, Germany), primer and probe design, quantitative Reverse Transcriptase-PCR (RT-qPCR) protocols, RT-qPCR and data analysis was performed as previously described [47].

Transcript expression levels of murine *Muc1, -2, -3, -4, -5ac, -5b* and *Muc6* were determined and normalized to the internal reference genes glyceraldehyde-3-phosphate dehydrogenase (*Gapdh*), elongationfactor 1α (*Ef-1α*) and ß-2 microglobulin (*B2m*) as previously described [47]. Primers and probes for *Ef-1α* [48], *Gapdh* [49], *B2m* [50], *Muc4* [51] and *Muc5ac* [52] were used as described. Primers and probes for *Muc1, -2, -3, -5b* and *-6* were designed using Primer3 software (WWW primertool, Whitehead Institute of Biomedical Research). Primer and probe sequences are listed in S6 Table.

The ΔΔCt method based on data obtained from naive WT control animals as reference allowed for relative expression level quantification and group comparison. Significance levels (p-values) were determined by Mann-Whitney-U test. Data are expressed as fold changes. Fold changes of 0.5 and 2 are considered as limits for valid statement of lowered and elevated parameters, respectively.

Statistics

Data are expressed as mean ± SEM, except for the proteomics log2 intensity, fecal microbiota composition and gene expression level data which are expressed as indicated. Pearson's correlation coefficient and the fraction of shared variance, R squared, were calculated for mucus proteomics data. Statistical analysis of mucus thickness and growth was performed with 2-way ANOVA followed by Tukey's HSD test for multiple comparisons. Impenetrable mucus thickness was compared by unpaired two-tailed t-test with 95% confidence interval. Other statistical analyses were performed using the Mann-Whitney-U test. $P < 0.05$ was considered significant. Statistical analysis and graphical illustrations were performed using GraphPad PRISM 6 (GraphPad Software Inc., La Jolla, USA).

Results

Expression of the major intestinal mucin Muc2 and mucus structure are not altered in *Clca1*^{-/-} mice

Previous studies have identified the highest levels of murine Clca1 expression as being located in the intestinal tract where it is restricted to mucin producing goblet cells in the upper half of

the colonic crypts and to villus goblet cells of the small intestine [10,13]. In order to investigate if Clca1 deficiency affected the Muc2 expression pattern or mucus structure in the large intestine, immunofluorescence (IF) using an anti-MUC2-C3 antibody was performed on sections from proximal, mid and distal colon. The anti-MUC2-C3 antibody failed to reveal any difference in staining patterns between the genotypes, neither in the crypt goblet cells nor in the secreted mucus (Fig 1A and 1B, green). Moreover, the stratified structures of the inner mucus were very similar (Fig 1B and 1i). These findings indicate normal Muc2 protein expression and mucus structure in *Clca1*^{-/-} mice. Staining with an anti-Clca1 antibody revealed, in contrast to previous data [13], a low expression of Clca1 in the proximal colon and higher expression in the distal colon (Fig 1A, red). We therefore focused the following experiments on the distal colon. The merged picture of Muc2 and Clca1 in WT confirmed co-localization of Clca1 to Muc2 producing goblet cells and presence of Clca1 in the secreted mucus (Fig 1A merge).

The specificity of the anti-CLCA1 antibody specificity was verified by staining *Clca1*^{-/-} distal colon sections as negative controls and comparing the staining pattern between antibodies directed against either the amino- or the carboxy terminus of Clca1 in WT sections (Fig 1C).

## Lack of Clca1 has no effect on the abundance of other proteins in the intestinal mucus

To study possible further effects of Clca1-deficiency on Muc2 and other important components of the mucus, such as Agr2, Fcgbp, Klk1 and Zg16, a proteomics study was performed. The relative abundances of proteins were compared in the mucus layer, displayed in a scatter plot showing a tight and significant correlation between WT and *Clca1*^{-/-} mucus proteins (Pearson´s r = 0.931, r^2 = 0.868, p < 0.0001, based on 809 valid pairs; Fig 2A). No significant differences in mucus protein expression were observed between the genotypes, except for the complete absence of the Clca1 protein in *Clca1*^{-/-} mice. The major mucus components Agr2, Fcgbp, Klk1 and Zg16 were also investigated by IF in distal colon sections with no differences found in their expression patterns or signal intensity between *Clca1*^{-/-} and wild type mice (Fig 2B).

Of the eight murine Clca family members, except for Clca1 in WT mice, only Clca4a and Clca4b (formerly known as mClca6 and mClca7, respectively, see revised nomenclature S1 Table) were identified in the mucus; however, they were only detected in a few samples with very few unique peptides and without any difference between the genotypes. The mass spectrometry proteomics data are presented in S7 Table and have been deposited to the ProteomeXchange Consortium with the dataset identifier PXD001804.

Mucus thickness, growth rate and impenetrability do not differ between WT and *Clca1*^{-/-} mice

The mucus phenotype of WT and *Clca1*^{-/-} mice was characterized in a set of *ex vivo* experiments examining the distal colonic mucus in which Clca1 is most abundantly detected.

Mucus was measured to investigate the initial thickness of the inner, firmly attached mucus as well as the secreted and expanding mucus over time both under normal and stimulated conditions. The outer, non-adherent mucus layer was flushed away prior to removal of the longitudinal muscle layer, providing an initial measurement representing the inner, adherent mucus thickness. Neither the thickness of the adherent mucus layer (65.3 ± 5.1 µm and 68.6 ± 5.8 µm for WT and *Clca1*^{-/-} mice, respectively; Fig 3A) nor the spontaneous mucus growth in the explant chamber system during 1 h (total thickness of 202.0 ± 15.8 µm and 180.7 ± 19.0 µm at t = 60 min with an average growth rate of 2.40 ± 0.21 µm/min and 1.89 ± 0.21 µm/min for WT and *Clca1*^{-/-} mice, respectively; Fig 3A and 3B) differed between the two genotypes. Increased mucus secretion was evident in both WT and *Clca1*^{-/-} tissue after addition of CCh, a cholinergic
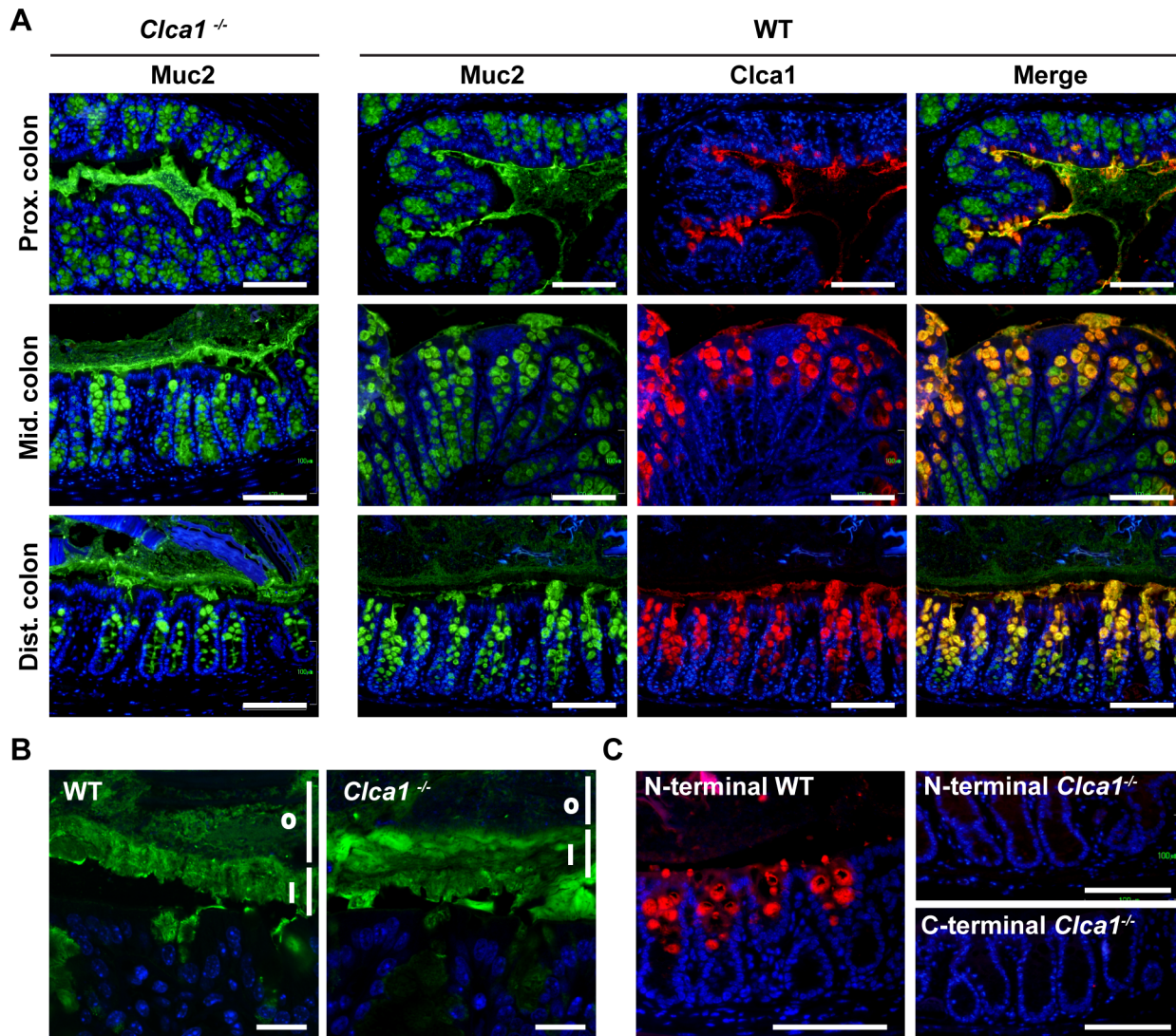
Fig 1. No difference of Muc2 expression pattern was observed by immunofluorescence in WT and *Clca1*⁻/⁻ mice. (A) The expression patterns of Muc2 (green) were investigated in the large intestine in *Clca1*⁻/⁻ mice and WT mice as control. No difference in Muc2 expression pattern could be detected between WT and *Clca1*⁻/⁻ mice in any location. Co-expression of Clca1 and Muc2 were confirmed by co-staining (yellow, merge with Clca1 carboxy-terminus stained red). The highest expression of CLCA1 was found in distal colon of WT mice and was restricted to goblet cells of the upper parts of the crypts. (B) Higher magnification revealed a stratified inner mucus layer by Muc2 staining (green) in both WT and *Clca1*⁻/⁻ distal colon sections. i = inner mucus layer, o = outer mucus layer. (C) Primary antibodies directed against either the amino- or carboxy-terminus of Clca1 (red) were used to confirm the absence of murine Clca1 expression in the distal colon of *Clca1*⁻/⁻ mice. All sections were stained with Hoechst 34580 DNA stain (blue), n = 4 per group. Scale bars in A and C 100 μm, in B 20 μm.

agonist known to induce intestinal epithelial ion and mucus secretion, and a significantly thicker mucus layer compared to unstimulated tissue was measured after a total of 60 min in the chamber (261.6 ± 20.0 μm vs. 202.0 ± 15.8 μm in WT, $p < 0.01$ and 258.1 ± 15.0 μm vs. 180.7 ± 19.0 μm in *Clca1*⁻/⁻ mice, $p < 0.01$; Fig 3A). No difference in total mucus thickness before and after CCh stimulation was noted between WT and *Clca1*⁻/⁻ mice (261.6 ± 20.0 μm vs. 258.1 ± 15.0 μm, respectively). The mucus growth rate showed an immediate peak response to CCh at 30–45 min in tissue explants of both genotypes (Fig 3B). The difference observed could indicate a small shift in peak response time that might be from variation in administration in the basolateral perfusate. In addition, a drop in the transepithelial potential difference,
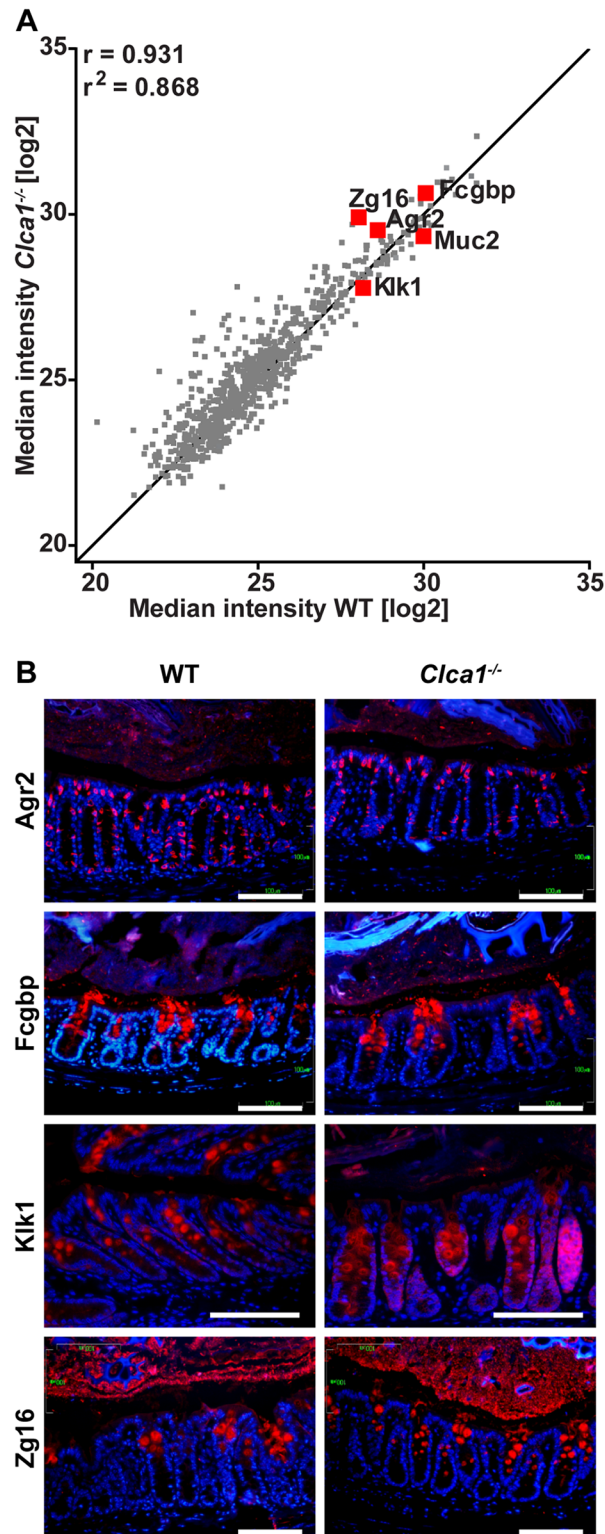
Fig 2. Major mucus components—Agr2, Fcgbp, Klk1, Muc2 and Zg16 –are unaltered in *Clca1*^{-/-} colonic mucus compared to WT controls. (A) Scatter plot depicting correlation in the median label-free intensity of all mucus proteins between WT and *Clca1*^{-/-} mice by proteome analysis using mass spectrometry with the correlation coefficient (Pearson's r) and r^2 shown. Proteins marked with red represent known major mucus components (Agr2, Fcgbp, Klk1, Muc2 and Zg16). Line = x + 1; n = 5 per group. (B) IF of Agr2, Fcgbp, Klk1 or

Zg16 (red) in WT and *Clca1*$^{-/-}$ distal colon sections, confirmed that there is no difference in protein expression in any of the major mucus proteins in *Clca1*$^{-/-}$ mice compared to WT, n = 2–3 per group. Blue = Hoechst 34580 DNA-stain, scale bars 100 μm.

indicating the presence of an ion transport, was noted concurrently with the increase in mucus growth rate both in WT and *Clca1*$^{-/-}$ mice.

To test whether Clca1 has any structural relevance for mucus barrier formation, a penetrability and distribution assay was performed in which bacteria-sized beads were applied on top of the mucus and their distribution in the mucus was investigated by confocal microscopy. Both in WT and in *Clca1*$^{-/-}$ mice, a clear separation between the epithelium and the beads sedimenting on top of the mucus was observed (Fig 3C). Impenetrable mucus thickness was the same for WT and *Clca1*$^{-/-}$ mice (115.0 ± 10.2 μm and 128.6 ± 8.1 μm in WT and *Clca1*$^{-/-}$ mice, respectively; Fig 3D). The exclusion of bacteria from the inner mucus layer was confirmed for both genotypes with FISH using a general bacterial probe and Muc2 counterstaining (Fig 3E).

The mucus barriers of WT and *Clca1*$^{-/-}$ mice are identically affected under DSS challenge

Mucus penetration and layering of the inner, stratified mucus layer and goblet cell filling were assessed via FISH and IF microscopy after 24 and 48 h of DSS application. Overall, the mucus penetrability increased significantly during DSS treatment from 1.1 ± 0.6 and 1.0 ± 0.5 (naive conditions) to 2.8 ± 0.4 and 2.9 ± 0.4 (24 h DSS) and to 3.4 ± 0.3 and 3.6 ± 0.3 (48 h DSS) for WT and *Clca1*$^{-/-}$ mice, respectively ($p < 0.01$ for all groups except WT naive vs. 24 h DSS $p < 0.05$; Fig 4A). This clearly reflects the expected loss of mucus barrier integrity within the first 48 h of DSS administration [28]; however, without any significant difference between the two genotypes.

The mucus layering score increased under the influence of DSS without any observable difference between the genotypes from 0.9 ± 0.4 and 0.8 ± 0.3 (naive conditions) to 1.9 ± 0.3 and 1.8 ± 0.3 (24 h DSS) and to 2.1 ± 0.2 and 1.8 ± 0.3 (48 h DSS) for WT and *Clca1*$^{-/-}$ mice, respectively ($p < 0.05$; Fig 4B), due to loss of mucus structure which correlates well with the penetration score.

The goblet cell filling score remained similar from 1.3 ± 0.3 and 1.0 ± 0.2 (naive conditions) to 1.0 ± 0.2 and 1.6 ± 0.2 (24 h DSS) and to 1.1 ± 0.1 and 0.6 ± 0.2 (48 h DSS) for WT and *Clca1*$^{-/-}$ mice, respectively. A significant increase in goblet cell filling was observed only at the single time point of 48 h for *Clca1*$^{-/-}$ compared to WT mice ($p < 0.05$; Fig 4C).

Loss of Clca1 has no effect on bacterial translocation in naive and DSS-challenged mice

In addition to characterizing bacterial mucus penetration via FISH, we also determined the relative translocation frequencies of live bacteria into selected sentinel organs such as blood, mesenteric lymph nodes, liver and spleen. Overall, there was neither a difference between the genotypes nor between naive and colitic mice of the same genotype (data not shown).

Fecal microbiota composition, blood content and stool consistency are not altered during acute colitis in WT and *Clca1*$^{-/-}$ mice

Since a change in intestinal microbiota composition gives rise to an altered chemical mucus composition and goblet cell function [53], we quantified selected species of the fecal microbiota
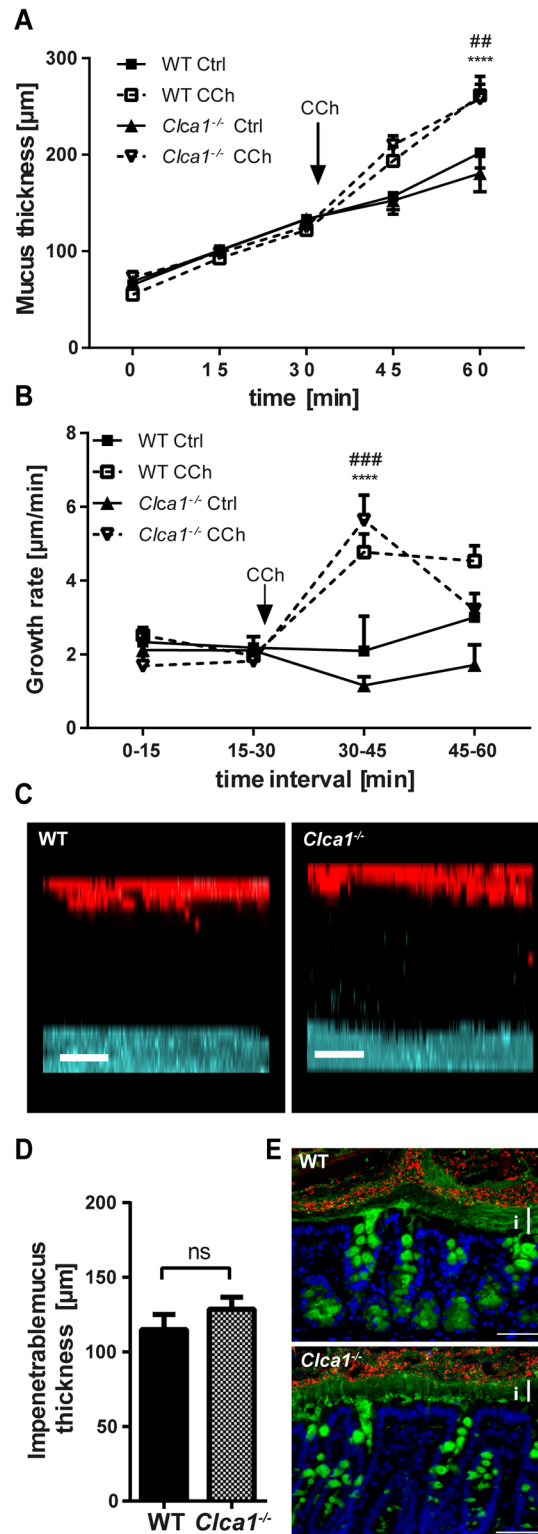
Fig 3. *Clca1*^{-/-} has no effect on mucus growth, responsiveness and penetrability in *Clca1*^{-/-} mice. (A) After flushing distal colon explants, mucus thickness and growth were similar in *Clca1*^{-/-} mice (dotted lines) compared to WT (filled lines). After CCh stimulation, an increase in mucus thickness compared to unstimulated explants was observed both in WT and in *Clca1*^{-/-} mice. Ctrl = control. (B) The growth rate was constant during unstimulated conditions whereas a significant growth rate increase in response to CCh was

evident in both groups shortly after its addition. No significant difference was observed between the groups. Ctrl = control. (C) *Ex vivo* mucus penetrability assessment using bacteria-sized beads (1 μm, red) and confocal microscopy was performed. Representative z-stack projections from WT and *Clca1⁻ᐟ⁻* mucus 30 minutes after tissue mounting both showed a clear separation between the tissue (blue) and the beads (red). Scale bars 50 μm. (D) The impenetrable mucus thickness, measured as the distance between the tissue and the sedimented beads in the confocal z-stacks did not differ between WT and *Clca1⁻ᐟ⁻* mice. ns = non-significant. (E) FISH with a general bacterial 16S probe (EUB338, red), counterstained for Muc2 (anti-MUC2-C3, green) and DNA (Hoechst 34580, blue) in sections from distal colon confirmed the impenetrability of the inner mucus layer both in WT and *Clca1⁻ᐟ⁻* mice with a clear separation of the tissue and bacteria. i = inner mucus layer. Scale bars 100 μm. n = 5 per group. Data are presented as mean ± SEM. $^{\#\#}$ p < 0.01, $^{\#\#\#}$ p < 0.001 for WT Ctrl vs. WT CCh; ****p < 0.0001 for *Clca1⁻ᐟ⁻* Ctrl vs. *Clca1⁻ᐟ⁻* CCh.

in colonic fecal samples of mice before and after treatment with DSS (7 d-group) by real-time PCR, with a comparison between WT and *Clca1⁻ᐟ⁻* mice (Fig 5A).

In the naive state, mice of either genotype had a very similar microbiota composition. Following colitis induction, increases in the colonic *Clostridium leptum* group and in the *Clostridium coccoides* group were statistically significant. Bifidobacteria were only detectable above the cut-off value of 10^0 gene copy numbers/ng DNA during colitis with no statistically significant difference between the genotypes.

Fecal blood content (Fig 5B) and stool consistency scores (Fig 5C) revealed an overall increase over the course of DSS administration, but without any statistically significant differences between genotypes, except for a higher fecal blood content score of WT vs. *Clca1⁻ᐟ⁻* mice at day 4.

## Clca1 deficiency has no effect on the mRNA expression of mucin genes under naive and DSS challenged conditions

After treatment with DSS for 24 or 48 h as well as for 7 d (n = 9–16 for each group), mRNA expression levels of selected mucin genes (*Muc1*, *2*, *3*, *4*, *5ac*, *5b* and *6*) were compared by RT-qPCR in distal colon samples to those of respective controls (Fig 6A–6D). *Muc1* gene expression (Fig 6A) did not show any statistically significant difference between the genotypes or between naive and DSS-challenged conditions.

Only in the 7 d-group was a statistically significant difference seen compared to water controls with *Muc2* and *Muc3* (Fig 6B and 6C, respectively) both down-regulated in WT (p < 0.05 and < 0.01, respectively) as well as in *Clca1⁻ᐟ⁻* mice (p < 0.05 and < 0.0001, respectively). Furthermore, a slightly lower expression of *Muc2* and slightly higher expression of *Muc3* was noted in *Clca1⁻ᐟ⁻* mice compared to WT mice under naive conditions which levelled out in the course of DSS challenge.

No significant differential expression was observed for *Muc4* (Fig 6D). Overall, *Muc5ac, -5b* and *-6* failed to show any relevant expression in the distal colon of WT and *Clca1⁻ᐟ⁻* mice under naive and DSS challenged conditions.

Discussion

CLCA1 is expressed and secreted by goblet cells in all investigated species so far including humans [9], mice [10], horses [54], and pigs [55] and is a major constituent of the intestinal mucus [10,11,13]. In CF knockout mice Clca1 expression is reduced [26] while experimental overexpression in CF ameliorates the murine intestinal mucus phenotype, characterized by mucus inspissation and intestinal obstruction [23]. A similar correlation has been found in humans where a certain allelic variant of CLCA1 is significantly overrepresented in CF patients with aggravated intestinal disease [56]. These observations have given rise to the hypothesis that Clca1 play a role in intestinal goblet cell function, mucus properties or modulation of
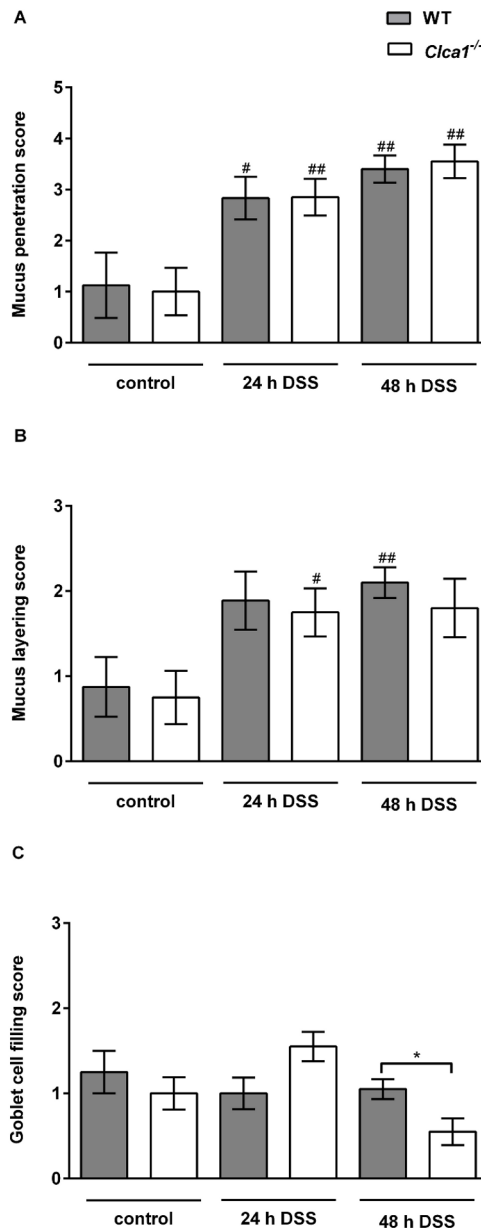
Fig 4. The mucus barrier of WT and *Clca1*⁻/⁻ mice are identically affected during DSS challenge. Mucus penetration, mucus layering and goblet cell filling in the colon of mice after 24 and 48 h DSS treatment were assessed using IF microscopy. (A) Mucus penetration increased identically under DSS treatment, however, without any significant difference between the genotypes. (B) The mucus layering score also increased under DSS influence without any observable difference between the genotypes. (C) The goblet cell filling score did not show any statistically significant differences, neither between genotypes nor between naive vs. DSS-treated animals, except for WT vs. *Clca1*⁻/⁻ mice after 48 hours. Mean values (n = 8 to 10). The scoring system is depicted in S3 Table and S4 Table. #p < 0.05 and ##p < 0.01 versus the naive control group. *p < 0.05 as indicated. Scale bars 50 μm.

doi:10.1371/journal.pone.0131991.g004

secretion [23]. Consequently, we also speculated that it may have an impact on the protective function of the intestinal mucus barrier.

    This study therefore focused on the characterization of the intestinal mucus phenotype in WT controls versus *Clca1*⁻/⁻ mice. The expression of Clca1, which colocalizes with Muc2
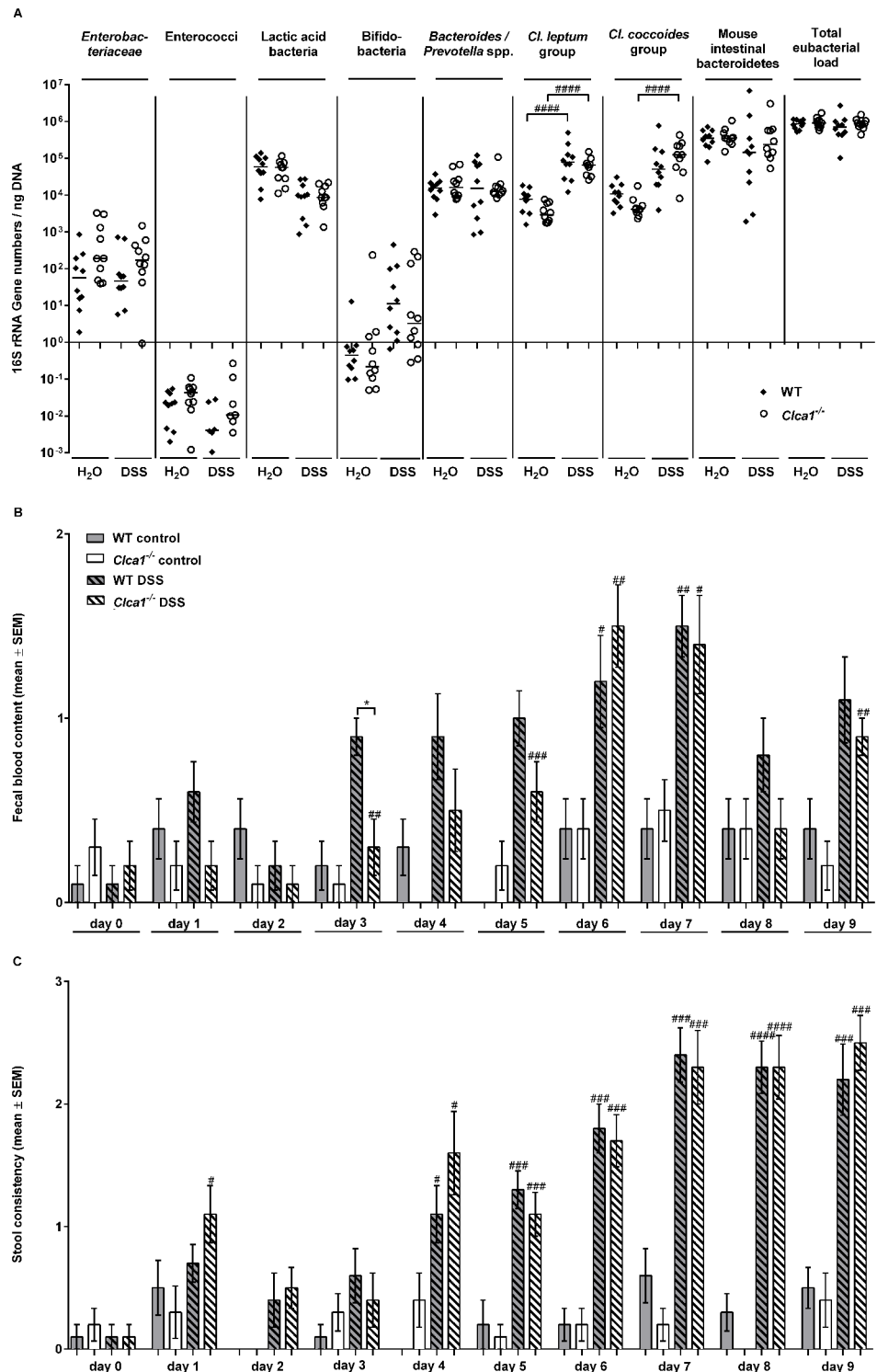
Fig 5. The fecal microbiota composition, blood content and stool consistency are altered during DSS-colitis without differences between *Clca1^-/-* and wild type mice. (A) Real-time-PCR analyses, amplifying bacterial 16S rRNA variable regions and 16S rRNA gene numbers/ng DNA derived from colon samples, were employed in order to analyze colonic microbiota composition regarding main intestinal bacterial groups—*Enterobacteriaceae*, enterococci, lactic acid bacteria, bifidobacteria, *Bacteroides/Prevotella* spp., *Clostridium leptum* group, *Clostridium coccoides* group, mouse intestinal bacteroidetes, and total eubacterial load—whilst comparing WT and *Clca1^-/-* fecal samples collected before and after DSS treatment (7 d-group). In the

naive state, mice of either genotype had a comparable fecal microbiota composition. Following colitis induction, increases in the colonic *Clostridium leptum* and *Clostridium coccoides* group as well as in bifidobacteria were evident, yet without any statistically significant difference between the genotypes. A minimum cut-off value of 10^0 gene copy numbers/ng DNA and a minimum log-change of 1 were set as limits of statistically significant relevance. Medians (n = 9 to 10) and significance levels (p values) determined by the Mann-Whitney-U test are indicated. ####p < 0.0001 vs. before DSS application. (B) Fecal blood content and (C) stool consistency scores revealed an overall increase in the course of DSS administration without any statistically significant differences between genotypes, except for a higher fecal blood content score in WT vs. *Clca1*⁻/⁻ mice at day 4. Mean values (n = 9 to 10) ± SEM and significance levels (p values) determined by the Mann-Whitney-U test are indicated. No boxplot = scores of all animals in this group were zero.
#p < 0.05, ##p < 0.1, ###p < 0.01 and ####p < 0.001 versus the naive control group. *p < 0.05 as indicated.

doi:10.1371/journal.pone.0131991.g005
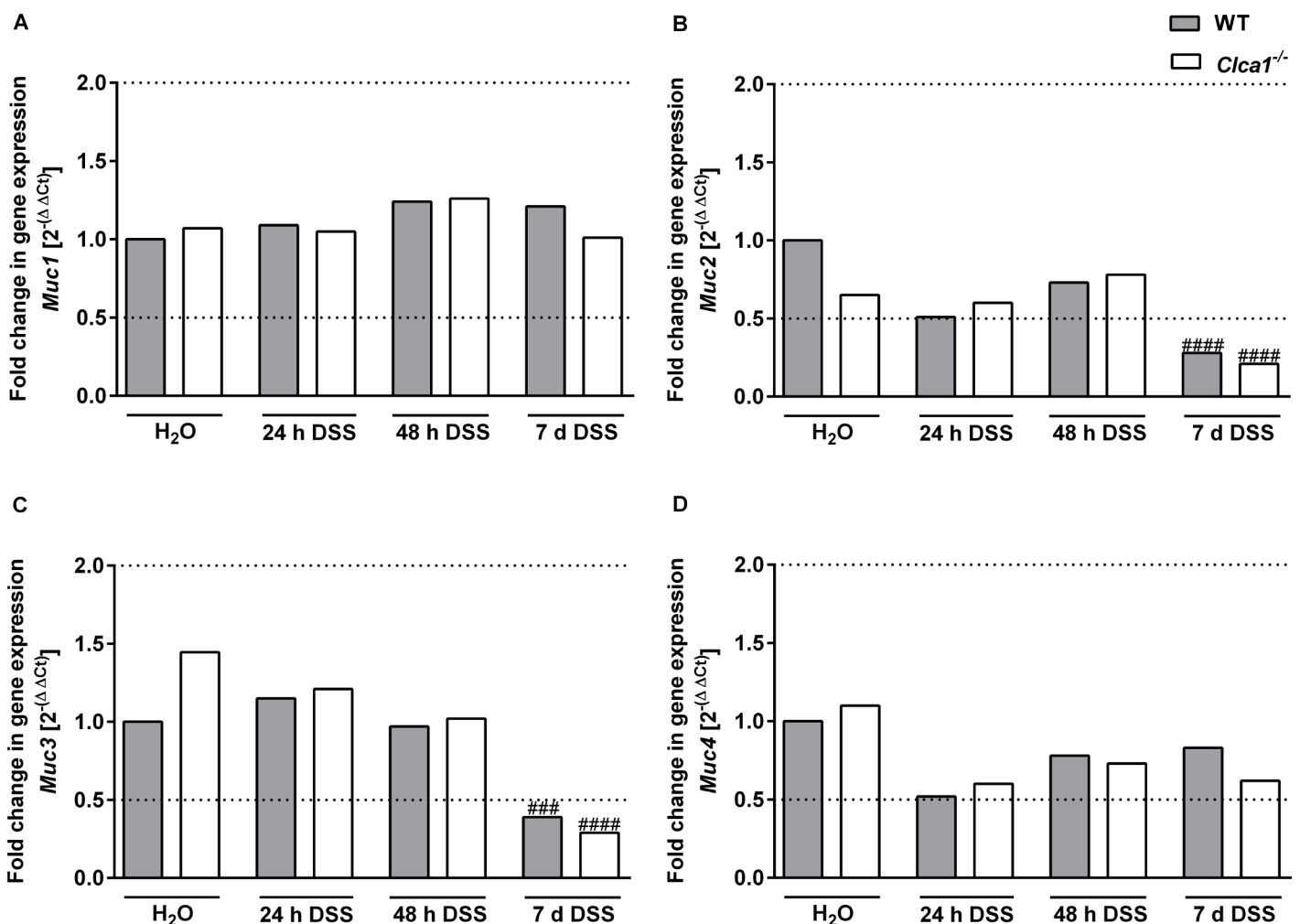
Fig 6. Clca1-deficiency has no effect on the mRNA expression of mucin genes in the intestinal tract under naive and DSS challenged conditions. After treatment of mice with DSS for 24 or 48 h as well as for 7 d with respective controls (n = 9–16 per group), mRNA expression levels of mucin genes were determined by quantitative RT-PCR. (A) *Muc1* gene expression did not show any statistically significant difference, neither between the genotypes nor during challenge. For (B) *Muc2* and (C) *Muc3*, a statistically significant down-regulation in WT and *Clca1*⁻/⁻ was seen in the 7 d-group compared to water controls. (D) *Muc4* also did not show any significant differential expression, neither between nor amongst the genotypes. Dotted lines indicate a fold change of 0.5 and 2, respectively, as limits for valid statement of lowered and elevated parameters. Ct, cycle threshold. ###p < 0.001 and ####p < 0.0001 vs. the naive control group.

doi:10.1371/journal.pone.0131991.g006

increases along the intestinal axis and thus parallels the increasing impenetrability of the mucus [57]. This also supported our hypothesis that CLCA1 may have a function in the intestinal mucus barrier.

Much to our surprise, the data presented here failed to reveal any involvement in normal mucus structure and function in the model and under the conditions used. No difference in mucus thickness, adherence to the epithelium or transformation from inner to outer mucus was observed between the genotypes, indicating normal mucus secretion and processing in the absence of Clca1. Additionally, an equal responsiveness to the secretagogue carbachol and quality of the mucus preventing bacterial penetration towards the epithelium was observed in *Clca1*^{-/-} and WT mice. The relative protein abundance and expression pattern of the main structural mucus component Muc2 and of other mucus proteins, such as Agr2, Klk1, Fcgbp, Zg16 were unaltered in the Clca1-deficient tissues. The proteomics data also failed to reveal significant changes in mucus composition of *Clca1*^{-/-} mice except for the lack of Clca1.

Our data analysis panel is well in line with and complements previous, solely histological investigations which failed to reveal any intestinal phenotype of various unchallenged *Clca1*^{-/-} models [52,58]. In addition to unchallenged conditions, we also tested for effects of lack of Clca1 in comparison to WT mice after DSS-challenge. The highly sulphated dextran of DSS has a dramatic and rapid destructive impact on the mucus structure and is commonly used as an inducer of colitis in mice [28,59]. Overall, the statistically significant bacterial penetrability increase between the respective naive and DSS-treated groups of the same genotype confirmed the expected loss of mucus barrier integrity within the first 48 h after initial DSS administration [28], but without any significant difference between the genotypes. The overall loss of layering structure within the first 48 h is also in line with previous observations [28]. The only statistically significant difference observed was the higher filling status of *Clca1*^{-/-} goblet cells after 48 h of DSS administration. This could either reflect a decreased mucus release in *Clca1*^{-/-} mice which is contradicted by the mucus structure analysis or may result from an increased synthesis which is contradicted by the gene expression data, both of which show no difference between the genotypes. We therefore feel that the statistical significance of the goblet cell filling score may be biologically debatable. However, we cannot exclude that Clca1 plays a role in exocytosis of mucin granules.

Furthermore, we quantified the induction of selected mucin genes in the distal colon. Mucins are subdivided into the goblet cell secreted gel-forming mucins such as Muc2, Muc5ac, Muc5b and Muc6 and the transmembrane mucins, expressed by epithelial cells, such as Muc1, Muc3 and Muc4 [60–62]. Of these Muc1 to 4 are expressed in the large intestine [63]. No significant alterations in intestinal mucin gene expression were observed between the genotypes in unchallenged conditions although a slightly lower expression of the secreted mucin *Muc2* and slightly higher expression of the membrane-bound *Muc3* were noted in *Clca1*^{-/-} mice compared to WT mice. This difference disappeared during the course of DSS application. In the 7 d-group, *Muc2* and *-3* were, in a very similar fashion, significantly down-regulated in WT and *Clca1*^{-/-} mice compared to water controls which is in line with decreased Muc2 mucin synthesis observed under pathological conditions [64]. It should also be mentioned that RNA levels often poorly correlate with protein levels in the mucus since goblet cells are capable of storing large amounts of mucus. We also failed to detect any changes in Muc2 expression along the intestinal tract by IF or in the relative abundance of Muc2 in the secreted mucus as observed by our proteomics data.

Muc5ac and 5b are the main respiratory mucins. Muc5ac is also expressed in the stomach and is transported through the intesinal tract [13] while MUC5B is expressed at low levels in human colon [65,66] but is not normally observed in the murine gastrointestinal tract [67,68]. MUC6 expression is normally restricted to the stomach and duodenum [69]. Muc5ac

expression was of particular interest due to its observed induction by CLCA1 overexpression in airway cell culture systems and in the respiratory tract [5,33]. In Crohn´s disease, MUC5AC expression is known to be induced in the intestine together with MUC5B and MUC6 [70]. Muc5ac is also expressed in the intestine upon clearance of helminth infections [71]. Besides Muc5ac, Muc6 was also of interest as it exhibited a transient *de novo*-expression in *Muc2*-deficient mice, possibly due to a compensatory protective mechanism within the colonic epithelium [72] although this has never been verified at protein level. In our study, *Muc5ac* and *-5b* as well as *Muc6* failed to show any significant expression in the distal colon, neither in the *Clca1*^{-/-} model nor during pathological conditions regardless of the genotype used. The lack of *Muc5ac*, *-5b* and *-6* on RNA-level is in line with previous reports that failed to detect these mucins at the protein level in unchallenged WT mice [13]. With this data we failed to observe any impact of *Clca1*-deficiency on mucin gene expression in the distal colon. Similar results had been obtained for the murine respiratory tract under naive and challenged conditions [47,52,58]. In contrast, it had been shown that human CLCA1 activates an Il-13-dependent MAPK-mediated airway mucin expression. These differences in mucin gene expression between mice and humans are perhaps due to compensatory effects of certain murine CLCA members [8]. It has previously been argued that, additionally to Clca1, the murine Clca2, -4a and -4b may also induce airway gene expression [8]. Of note, Clca4a and -4b have previously been found to be upregulated at the mRNA level in *Clca1*^{-/-} mice [52]. Here, however, only minute traces of Clca4a and -4b were identified in the secreted mucus without any difference between the genotypes. Clca4a is known to be expressed by enterocytes and its amino-terminal part is released into the mucus [21]. Clca4b is also expressed in the intestine [52,73]. However, its expressing cell type is unknown to date. The Clca2 protein which is expressed in keratinocytes of stratified epithelia and in distinct niches of the respiratory tract [48,74] has not been detected in the intestinal tract to date which is consistent with our findings [48]. The absence of any differential Clca expression pattern in the mucus on the protein level suggests that the lack of a phenotype may not be due to a phenotype rescue by other Clca homologs.

Intestinal microbiota composition was investigated with a focus on main gut bacterial groups which are known to be altered during colitis development [30,44]. After induction of acute DSS colitis, an increase in the colonic clostridia and bifidobacteria was observed which is consistent with previous findings, yet without significant differences between the genotypes [30]. The expected increased scores of fecal blood content and stool consistency, monitored as clinical parameters of colitis occurred independently of the genotype [34,35].

Taken together our data point towards a function of CLCA1 other than in mucus structure, function and barrier integrity. As an alternative function a role for CLCA1 as a signaling molecule regulating cytokine expression has become the focus of recent research. In the respiratory tract, *Clca1*^{-/-} mice develop decreased levels of Cxcl-1, a potent neutrophil chemoattractant [75,76], and of Il-17, a proinflammatory cytokine [77] at the mRNA and protein levels with a consequent decrease in neutrophil response during *Staphylococcus aureus* pneumonia [47]. This observation is in line with reduced Clca1 and CXCL-1 in an IL-17 neutralization study [78]. Consistent with this notion is that the human CLCA1 presumably induces a proinflammatory macrophage response [79]. It has therefore been speculated that CLCA1 may play a role in the modulation of an innate immunity response or cytokine regulation. As a second possible function it has been suggested that CLCA1 may play a role in the differentiation and proliferation of intestinal epithelial cells and colorectal cancer cells [80,81]. Finally, it was recently discovered that secreted CLCA1 increases the surface expression of TMEM16A (Anoctamin1/DOG1), the first genuine calcium-activated chloride channel, in a paracrine fashion and thereby increases the calcium-dependent chloride current *in vitro* [82]. Future experiments will have to clarify whether and how CLCA1 actually fulfills and possibly even

combines several of these suggested functions and how they may relate to the proposed roles of CLCA1 in maladies with secretory dysfunctions. A role for CLCA1 as a signaling molecule affecting the integrity of the epithelial barrier could also be a new area of interest. In conclusion, our results show that Clca1 is not required for intestinal mucus synthesis, structure and barrier function in naive or DSS-challenged mice.

Supporting Information

S1 Table. Revised CLCA nomenclature.
(PDF)

S2 Table. Scoring system for bacterial penetration of the inner mucus layer.
(PDF)

S3 Table. Scoring examples for the inner mucus layer.
(PDF)

S4 Table. Scoring system for the goblet cell filling.
(PDF)

S5 Table. 16S rRNA gene group-specific primers for quantitative Real Time-PCR.
(PDF)

S6 Table. Primers and probes for quantitative Real Time-PCR.
(PDF)

S7 Table. Mucus proteome in wild type and *Clca1*^{-/-} distal colon.
(PDF)

Acknowledgments

Author Contributions

Conceived and designed the experiments: NAE EELN LM RG MMH AF SB ADG MEVJ. Performed the experiments: NAE EELN LM LA RG MMH AF GMHB. Analyzed the data: NAE EELN LM LA MMH AF GMHB MEVJ. Contributed reagents/materials/analysis tools: RG AF MMH SB ADG MEVJ. Wrote the paper: NAE EELN LM LA MMH AF SB GMHB ADG MEVJ.

References

1. Toda M, Tulic MK, Levitt RC, Hamid Q. A calcium-activated chloride channel (HCLCA1) is strongly related to IL-9 expression and mucus production in bronchial epithelium of patients with asthma. J Allergy Clin Immunol 2002 Feb; 109(2):246–50. PMID: 11842292

2. Hauber HP, Tsicopoulos A, Wallaert B, Griffin S, McElvaney NG, Daigneault P, et al. Expression of HCLCA1 in cystic fibrosis lungs is associated with mucus overproduction. Eur Respir J 2004 Jun; 23 (6):846–50. PMID: 15218996

3. Hegab AE, Sakamoto T, Uchida Y, Nomura A, Ishii Y, Morishima Y, et al. CLCA1 gene polymorphisms in chronic obstructive pulmonary disease. J Med Genet 2004 Mar; 41(3):e27. PMID: 14985398

4. Patel AC, Brett TJ, Holtzman MJ. The role of CLCA proteins in inflammatory airway disease. Annu Rev Physiol 2009; 71:425–49. doi: 10.1146/annurev.physiol.010908.163253 PMID: 18954282

5. Nakanishi A, Morita S, Iwashita H, Sagiya Y, Ashida Y, Shirafuji H, et al. Role of gob-5 in mucus over-production and airway hyperresponsiveness in asthma. Proc Natl Acad Sci U S A 2001 Apr 24; 98 (9):5175–80. PMID: 11296262

6. Zhou Y, Dong Q, Louahed J, Dragwa C, Savio D, Huang M, et al. Characterization of a calcium-activated chloride channel as a shared target of Th2 cytokine pathways and its potential involvement in asthma. Am J Respir Cell Mol Biol 2001 Oct; 25(4):486–91. PMID: 11694454

7. Song L, Liu D, Wu C, Wu S, Yang J, Ren F, et al. Antibody to mCLCA3 suppresses symptoms in a mouse model of asthma. PLoS ONE 2013; 8(12):e82367. doi: 10.1371/journal.pone.0082367 PMID: 24349268

8. Alevy YG, Patel AC, Romero AG, Patel DA, Tucker J, Roswit WT, et al. IL-13-induced airway mucus production is attenuated by MAPK13 inhibition. J Clin Invest 2012 Dec 3; 122(12):4555–68. doi: 10. 1172/JCI64896 PMID: 23187130

9. Gruber AD, Elble RC, Ji HL, Schreur KD, Fuller CM, Pauli BU. Genomic cloning, molecular characterization, and functional analysis of human CLCA1, the first human member of the family of Ca2+-activated Cl- channel proteins. Genomics 1998 Dec 1; 54(2):200–14. PMID: 9828122

10. Leverkoehne I, Gruber AD. The murine mCLCA3 (alias gob-5) protein is located in the mucin granule membranes of intestinal, respiratory, and uterine goblet cells. J Histochem Cytochem 2002 Jun; 50 (6):829–38. PMID: 12019299

11. Johansson ME, Phillipson M, Petersson J, Velcich A, Holm L, Hansson GC. The inner of the two Muc2 mucin-dependent mucus layers in colon is devoid of bacteria. Proc Natl Acad Sci U S A 2008 Sep 30; 105(39):15064–9. doi: 10.1073/pnas.0803124105 PMID: 18806221

12. Agnel M, Vermat T, Culouscou JM. Identification of three novel members of the calcium-dependent chloride channel (CaCC) family predominantly expressed in the digestive tract and trachea. FEBS Lett 1999 Jul 23; 455(3):295–301. PMID: 10437792

13. Rodriguez-Pineiro AM, Bergstrom JH, Ermund A, Gustafsson JK, Schutte A, Johansson ME, et al. Studies of mucus in mouse stomach, small intestine, and colon. II. Gastrointestinal mucus proteome reveals Muc2 and Muc5ac accompanied by a set of core proteins. Am J Physiol Gastrointest Liver Physiol 2013 Sep 1; 305(5):G348–G356. doi: 10.1152/ajpgi.00047.2013 PMID: 23832517

14. Ambort D, Johansson ME, Gustafsson JK, Ermund A, Hansson GC. Perspectives on mucus properties and formation—lessons from the biochemical world. Cold Spring Harb Perspect Med 2012 Nov; 2(11).

15. Johansson ME, Sjovall H, Hansson GC. The gastrointestinal mucus system in health and disease. Nat Rev Gastroenterol Hepatol 2013 Jun; 10(6):352–61. doi: 10.1038/nrgastro.2013.35 PMID: 23478383

16. Johansson ME, Gustafsson JK, Holmen-Larsson J, Jabbar KS, Xia L, Xu H, et al. Bacteria penetrate the normally impenetrable inner colon mucus layer in both murine colitis models and patients with ulcerative colitis. Gut 2014 Feb; 63(2):281–91. doi: 10.1136/gutjnl-2012-303207 PMID: 23426893

17. Fu J, Wei B, Wen T, Johansson ME, Liu X, Bradford E, et al. Loss of intestinal core 1-derived O-glycans causes spontaneous colitis in mice. J Clin Invest 2011 Apr 1; 121(4):1657–66. doi: 10.1172/JCI45538 PMID: 21383503

18. Carvalho FA, Koren O, Goodrich JK, Johansson ME, Nalbantoglu I, Aitken JD, et al. Transient inability to manage proteobacteria promotes chronic gut inflammation in TLR5-deficient mice. Cell Host Microbe 2012 Aug 16; 12(2):139–52. doi: 10.1016/j.chom.2012.07.004 PMID: 22863420

19. Yurtsever Z, Sala-Rabanal M, Randolph DT, Scheaffer SM, Roswit WT, Alevy YG, et al. Self-cleavage of human CLCA1 protein by a novel internal metalloprotease domain controls calcium-activated chloride channel activation. J Biol Chem 2012 Dec 7; 287(50):42138–49. doi: 10.1074/jbc.M112.410282 PMID: 23112050

20. Pawlowski K, Lepisto M, Meinander N, Sivars U, Varga M, Wieslander E. Novel conserved hydrolase domain in the CLCA family of alleged calcium-activated chloride channels. Proteins 2006 May 15; 63 (3):424–39. PMID: 16470849

21. Bothe MK, Mundhenk L, Kaup M, Weise C, Gruber AD. The murine goblet cell protein mCLCA3 is a zinc-dependent metalloprotease with autoproteolytic activity. Mol Cells 2011 Dec; 32(6):535–41. doi: 10.1007/s10059-011-0158-8 PMID: 22080371

22. Mundhenk L, Alfalah M, Elble RC, Pauli BU, Naim HY, Gruber AD. Both cleavage products of the mCLCA3 protein are secreted soluble proteins. J Biol Chem 2006 Oct 6; 281(40):30072–80. PMID: 16895902

23. Young FD, Newbigging S, Choi C, Keet M, Kent G, Rozmahel RF. Amelioration of cystic fibrosis intestinal mucous disease in mice by restoration of mCLCA3. Gastroenterology 2007 Dec; 133(6):1928–37. PMID: 18054564

24. Gibson A, Lewis AP, Affleck K, Aitken AJ, Meldrum E, Thompson N. hCLCA1 and mCLCA3 are secreted non-integral membrane proteins and therefore are not ion channels. J Biol Chem 2005 Jul 22; 280(29):27205–12. PMID: 15919655

25. Whittaker CA, Hynes RO. Distribution and evolution of von Willebrand/integrin A domains: widely dispersed domains with roles in cell adhesion and elsewhere. Mol Biol Cell 2002 Oct; 13(10):3369–87. PMID: 12388743

26. Brouillard F, Bensalem N, Hinzpeter A, Tondelier D, Trudel S, Gruber AD, et al. Blue native/SDS-PAGE analysis reveals reduced expression of the mClCA3 protein in cystic fibrosis knock-out mice. Mol Cell Proteomics 2005 Nov; 4(11):1762–75. PMID: 16099848

27. Hoshino M, Morita S, Iwashita H, Sagiya Y, Nagi T, Nakanishi A, et al. Increased expression of the human Ca2+-activated Cl- channel 1 (CaCC1) gene in the asthmatic airway. Am J Respir Crit Care Med 2002 Apr 15; 165(8):1132–6. PMID: 11956057

28. Johansson ME, Gustafsson JK, Sjoberg KE, Petersson J, Holm L, Sjovall H, et al. Bacteria Penetrate the Inner Mucus Layer before Inflammation in the Dextran Sulfate Colitis Model. PLoS ONE 2010; 5(8): e12238. doi: 10.1371/journal.pone.0012238 PMID: 20805871

29. Perse M, Cerar A. Dextran sodium sulphate colitis mouse model: traps and tricks. J Biomed Biotechnol 2012; 2012:718617. doi: 10.1155/2012/718617 PMID: 22665990

30. Heimesaat MM, Fischer A, Siegmund B, Kupz A, Niebergall J, Fuchs D, et al. Shift towards pro-inflammatory intestinal bacteria aggravates acute murine colitis via Toll-like receptors 2 and 4. PLoS ONE 2007; 2(7):e662. PMID: 17653282

31. Lupp C, Robertson ML, Wickham ME, Sekirov I, Champion OL, Gaynor EC, et al. Host-mediated inflammation disrupts the intestinal microbiota and promotes the overgrowth of Enterobacteriaceae. Cell Host Microbe 2007 Aug 16; 2(2):119–29. PMID: 18005726

32. Mahler CM, Berard M, Feinstein R, Gallagher A, Illgen-Wilcke B, Pritchett-Corning K, et al. FELASA recommendations for the health monitoring of mouse, rat, hamster, guinea pig and rabbit colonies in breeding and experimental units. Lab Anim 2014 Feb 4; 48(3):178–92. PMID: 24496575

33. Patel AC, Morton JD, Kim EY, Alevy Y, Swanson S, Tucker J, et al. Genetic segregation of airway disease traits despite redundancy of calcium-activated chloride channel family members. Physiol Genomics 2006 May 16; 25(3):502–13. PMID: 16569774

34. Byrnes JJ, Gross S, Ellard C, Connolly K, Donahue S, Picarella D. Effects of the ACE2 inhibitor GL1001 on acute dextran sodium sulfate-induced colitis in mice. Inflamm Res 2009 Nov; 58(11):819–27. doi: 10.1007/s00011-009-0053-3 PMID: 19517214

35. Wirtz S, Neufert C, Weigmann B, Neurath MF. Chemically induced mouse models of intestinal inflammation. Nat Protoc 2007; 2(3):541–6. PMID: 17406617

36. Johansson ME, Hansson GC. Preservation of Mucus in Histological Sections, Immunostaining of Mucins in Fixed Tissue, and Localization of Bacteria with FISH. Methods Mol Biol 2012; 842:229–35. doi: 10.1007/978-1-61779-513-8_13 PMID: 22259139

37. Gustafsson JK, Ermund A, Johansson ME, Schutte A, Hansson GC, Sjovall H. An ex vivo method for studying mucus formation, properties, and thickness in human colonic biopsies and mouse small and large intestinal explants. Am J Physiol Gastrointest Liver Physiol 2012 Feb; 302(4):G430–G438. doi: 10.1152/ajpgi.00405.2011 PMID: 22159279

38. Wisniewski JR, Zougman A, Nagaraj N, Mann M. Universal sample preparation method for proteome analysis. Nat Methods 2009 May; 6(5):359–62. doi: 10.1038/nmeth.1322 PMID: 19377485

39. van der Post S, Hansson GC. Membrane protein profiling of human colon reveals distinct regional differences. Mol Cell Proteomics 2014 Sep; 13(9):2277–87. doi: 10.1074/mcp.M114.040204 PMID: 24889196

40. Cox J, Mann M. MaxQuant enables high peptide identification rates, individualized p.p.b.-range mass accuracies and proteome-wide protein quantification. Nat Biotechnol 2008 Dec; 26(12):1367–72. doi: 10.1038/nbt.1511 PMID: 19029910

41. Vizcaino JA, Deutsch EW, Wang R, Csordas A, Reisinger F, Rios D, et al. ProteomeXchange provides globally coordinated proteomics data submission and dissemination. Nat Biotechnol 2014 Mar; 32 (3):223–6. doi: 10.1038/nbt.2839 PMID: 24727771

42. Bereswill S, Munoz M, Fischer A, Plickert R, Haag LM, Otto B, et al. Anti-inflammatory effects of resveratrol, curcumin and simvastatin in acute small intestinal inflammation. PLoS ONE 2010; 5(12):e15099. doi: 10.1371/journal.pone.0015099 PMID: 21151942

43. Heimesaat MM, Bereswill S, Fischer A, Fuchs D, Struck D, Niebergall J, et al. Gram-negative bacteria aggravate murine small intestinal Th1-type immunopathology following oral infection with Toxoplasma gondii. J Immunol 2006 Dec 15; 177(12):8785–95. PMID: 17142781

44. Heimesaat MM, Nogai A, Bereswill S, Plickert R, Fischer A, Loddenkemper C, et al. MyD88/TLR9 mediated immunopathology and gut microbiota dynamics in a novel murine model of intestinal graft-versus-host disease. Gut 2010 Aug; 59(8):1079–87. doi: 10.1136/gut.2009.197434 PMID: 20639251

45. Rausch S, Held J, Fischer A, Heimesaat MM, Kuhl AA, Bereswill S, et al. Small intestinal nematode infection of mice is associated with increased enterobacterial loads alongside the intestinal tract. PLoS ONE 2013; 8(9):e74026. doi: 10.1371/journal.pone.0074026 PMID: 24040152

46. Thoene-Reineke C, Fischer A, Friese C, Briesemeister D, Gobel UB, Kammertoens T, et al. Composition of intestinal microbiota in immune-deficient mice kept in three different housing conditions. PLoS ONE 2014; 9(11):e113406. doi: 10.1371/journal.pone.0113406 PMID: 25401702

47. Dietert K, Reppe K, Mundhenk L, Witzenrath M, Gruber AD. mCLCA3 modulates IL-17 and CXCL-1 induction and leukocyte recruitment in murine Staphylococcus aureus pneumonia. PLoS ONE 2014; 9(7):e102606. doi: 10.1371/journal.pone.0102606 PMID: 25033194

48. Braun J, Mundhenk L, Range F, Gruber AD. Quantitative expression analyses of candidates for alternative anion conductance in cystic fibrosis mouse models. J Cyst Fibros 2010 Sep; 9(5):351–64. doi: 10.1016/j.jcf.2010.06.003 PMID: 20624691

49. Giulietti A, Overbergh L, Valckx D, Decallonne B, Bouillon R, Mathieu C. An overview of real-time quantitative PCR: applications to quantify cytokine gene expression. Methods 2001 Dec; 25(4):386–401. PMID: 11846608

50. Norris MD, Burkhart CA, Marshall GM, Weiss WA, Haber M. Expression of N-myc and MRP genes and their relationship to N-myc gene dosage and tumor formation in a murine neuroblastoma model. Med Pediatr Oncol 2000 Dec; 35(6):585–9. PMID: 11107123

51. Tetaert D, Pierre M, Demeyer D, Husson MO, Beghin L, Galabert C, et al. Dietary n-3 fatty acids have suppressive effects on mucin upregulation in mice infected with Pseudomonas aeruginosa. Respir Res 2007; 8:39. PMID: 17550583

52. Mundhenk L, Johannesson B, Anagnostopoulou P, Braun J, Bothe MK, Schultz C, et al. mCLCA3 does not contribute to calcium-activated chloride conductance in murine airways. Am J Respir Cell Mol Biol 2012 Jul; 47(1):87–93. doi: 10.1165/rcmb.2010-0508OC PMID: 22362387

53. Deplancke B, Gaskins HR. Microbial modulation of innate defense: goblet cells and the intestinal mucus layer. Am J Clin Nutr 2001 Jun; 73(6):1131S–41S. PMID: 11393191

54. Range F, Mundhenk L, Gruber AD. A soluble secreted glycoprotein (eCLCA1) is overexpressed due to goblet cell hyperplasia and metaplasia in horses with recurrent airway obstruction. Vet Pathol 2007 Nov; 44(6):901–11. PMID: 18039903

55. Plog S, Mundhenk L, Klymiuk N, Gruber AD. Genomic, tissue expression, and protein characterization of pCLCA1, a putative modulator of cystic fibrosis in the pig. J Histochem Cytochem 2009 Dec; 57(12):1169–81. doi: 10.1369/jhc.2009.954594 PMID: 19755716

56. van der Doef HP, Slieker MG, Staab D, Alizadeh BZ, Seia M, Colombo C, et al. Association of the CLCA1 p.S357N variant with meconium ileus in European patients with cystic fibrosis. J Pediatr Gastroenterol Nutr 2010 Mar; 50(3):347–9. doi: 10.1097/MPG.0b013e3181afce6c PMID: 20179644

57. Ermund A, Schutte A, Johansson ME, Gustafsson JK, Hansson GC. Studies of mucus in mouse stomach, small intestine, and colon. I. Gastrointestinal mucus layers have different properties depending on location as well as over the Peyer's patches. Am J Physiol Gastrointest Liver Physiol 2013 Sep 1; 305(5):G341–G347. doi: 10.1152/ajpgi.00046.2013 PMID: 23832518

58. Robichaud A, Tuck SA, Kargman S, Tam J, Wong E, Abramovitz M, et al. Gob-5 is not essential for mucus overproduction in preclinical murine models of allergic asthma. Am J Respir Cell Mol Biol 2005 Sep; 33(3):303–14. PMID: 15947424

59. Okayasu I, Hatakeyama S, Yamada M, Ohkusa T, Inagaki Y, Nakaya R. A novel method in the induction of reliable experimental acute and chronic ulcerative colitis in mice. Gastroenterology 1990 Mar; 98(3):694–702. PMID: 1688816

60. Rose MC, Voynow JA. Respiratory tract mucin genes and mucin glycoproteins in health and disease. Physiol Rev 2006 Jan; 86(1):245–78. PMID: 16371599

61. Hoebler C, Gaudier E, De CP, Rival M, Cherbut C. MUC genes are differently expressed during onset and maintenance of inflammation in dextran sodium sulfate-treated mice. Dig Dis Sci 2006 Feb; 51(2):381–9. PMID: 16534686

62. Johansson ME, Ambort D, Pelaseyed T, Schutte A, Gustafsson JK, Ermund A, et al. Composition and functional role of the mucus layers in the intestine. Cell Mol Life Sci 2011 Nov; 68(22):3635–41. doi: 10.1007/s00018-011-0822-3 PMID: 21947475

63. Corfield AP, Myerscough N, Longman R, Sylvester P, Arul S, Pignatelli M. Mucins and mucosal protection in the gastrointestinal tract: new prospects for mucins in the pathology of gastrointestinal disease. Gut 2000 Oct; 47(4):589–94. PMID: 10986224

64. Tytgat KM, van der Wal JW, Einerhand AW, Buller HA, Dekker J. Quantitative analysis of MUC2 synthesis in ulcerative colitis. Biochem Biophys Res Commun 1996 Jul 16; 224(2):397–405. PMID: 8702401

65. Van Klinken BJ, Dekker J, van Gool SA, van MJ, Buller HA, Einerhand AW. MUC5B is the prominent mucin in human gallbladder and is also expressed in a subset of colonic goblet cells. Am J Physiol 1998 May; 274(5 Pt 1):G871–G878. PMID: 9612268

66. Larsson JM, Karlsson H, Crespo JG, Johansson ME, Eklund L, Sjovall H, et al. Altered O-glycosylation profile of MUC2 mucin occurs in active ulcerative colitis and is associated with increased inflammation. Inflamm Bowel Dis 2011 Nov; 17(11):2299–307. doi: 10.1002/ibd.21625 PMID: 21290483

67. Escande F, Porchet N, Bernigaud A, Petitprez D, Aubert JP, Buisine MP. The mouse secreted gel-forming mucin gene cluster. Biochim Biophys Acta 2004 Feb 20; 1676(3):240–50. PMID: 14984930

68. Johansson ME, Thomsson KA, Hansson GC. Proteomic analyses of the two mucus layers of the colon barrier reveal that their main component, the Muc2 mucin, is strongly bound to the Fcgbp protein. J Proteome Res 2009 Jul; 8(7):3549–57. doi: 10.1021/pr9002504 PMID: 19432394

69. Desseyn JL, Laine A. Characterization of mouse muc6 and evidence of conservation of the gel-forming mucin gene cluster between human and mouse. Genomics 2003 Apr; 81(4):433–6. PMID: 12676567

70. Buisine MP, Desreumaux P, Leteurtre E, Copin MC, Colombel JF, Porchet N, et al. Mucin gene expression in intestinal epithelial cells in Crohn's disease. Gut 2001 Oct; 49(4):544–51. PMID: 11559653

71. Hasnain SZ, McGuckin MA, Grencis RK, Thornton DJ. Serine protease(s) secreted by the nematode Trichuris muris degrade the mucus barrier. PLoS Negl Trop Dis 2012 Oct; 6(10):e1856. doi: 10.1371/journal.pntd.0001856 PMID: 23071854

72. Van der SM, de Koning BA, De Bruijn AC, Velcich A, Meijerink JP, Van Goudoever JB, et al. Muc2-deficient mice spontaneously develop colitis, indicating that MUC2 is critical for colonic protection. Gastroenterology 2006 Jul; 131(1):117–29. PMID: 16831596

73. Al-Jumaily M, Kozlenkov A, Mechaly I, Fichard A, Matha V, Scamps F, et al. Expression of three distinct families of calcium-activated chloride channel genes in the mouse dorsal root ganglion. Neurosci Bull 2007 Sep; 23(5):293–9. PMID: 17952139

74. Dietert K, Mundhenk L, Erickson NA, Reppe K, Hocke AC, Kummer W, et al. Murine CLCA5 is uniquely expressed in distinct niches of airway epithelial cells. Histochem Cell Biol 2015 Mar; 143(3):277–87. doi: 10.1007/s00418-014-1279-x PMID: 25212661

75. Luster AD. Chemokines—chemotactic cytokines that mediate inflammation. N Engl J Med 1998 Feb 12; 338(7):436–45. PMID: 9459648

76. Huang S, Paulauskis JD, Godleski JJ, Kobzik L. Expression of macrophage inflammatory protein-2 and KC mRNA in pulmonary inflammation. Am J Pathol 1992 Oct; 141(4):981–8. PMID: 1415488

77. Korn T, Bettelli E, Oukka M, Kuchroo VK. IL-17 and Th17 Cells. Annu Rev Immunol 2009; 27:485–517. doi: 10.1146/annurev.immunol.021908.132710 PMID: 19132915

78. Mukherjee S, Lindell DM, Berlin AA, Morris SB, Shanley TP, Hershenson MB, et al. IL-17-induced pulmonary pathogenesis during respiratory viral infection and exacerbation of allergic disease. Am J Pathol 2011 Jul; 179(1):248–58. doi: 10.1016/j.ajpath.2011.03.003 PMID: 21703407

79. Ching JC, Lobanova L, Loewen ME. Secreted hCLCA1 is a signaling molecule that activates airway macrophages. PLoS ONE 2013; 8(12):e83130. doi: 10.1371/journal.pone.0083130 PMID: 24349445

80. Yang B, Cao L, Liu B, McCaig CD, Pu J. The transition from proliferation to differentiation in colorectal cancer is regulated by the calcium activated chloride channel A1. PLoS ONE 2013; 8(4):e60861. doi: 10.1371/journal.pone.0060861 PMID: 23593331

81. Yang B, Cao L, Liu J, Xu Y, Milne G, Chan W, et al. Low expression of chloride channel accessory 1 predicts a poor prognosis in colorectal cancer. Cancer 2015 Jan 20.

82. Sala-Rabanal M, Yurtsever Z, Nichols CG, Brett TJ. Secreted CLCA1 modulates TMEM16A to activate Ca-dependent chloride currents in human cells. Elife 2015; 4.